EJNMMI Radiopharmacy and Chemistry

RESEARCH ARTICLE Open Access

Exploring a tristhione scorpionate ligand as a suitable chelator for the theranostic pair antimony-119 and antimony-117

Lorraine Gaenaelle Gé[1,2], Mads Sondrup Møller[3], Catherine Chen[3], Virginia Cendán Castillo[3], Niels Langkjaer[1], Vickie McKee[4], Johan Hygum Dam[1,2], Christine J. McKenzie[3†] and Helge Thisgaard[1,2*†]

†Christine J. McKenzie and Helge Thisgaard are shared last authorship.

*Correspondence:
Helge Thisgaard
Helge.Thisgaard@rsyd.dk
[1]Department of Nuclear Medicine, Odense University Hospital, Kløvervaenget 47, Odense DK-5000, Denmark
[2]Department of Clinical Research, University of Southern Denmark, Odense, Denmark
[3]Department of Physics, Chemistry and Pharmacy, University of Southern Denmark, Odense, Denmark
[4]School of Chemical Sciences, Dublin City University, Glasnevin, Dublin 9, Ireland

Abstract

Background The highly potent Auger electron emitter antimony-119 (^{119}Sb) and the SPECT-isotope antimony-117 (^{117}Sb) comprise a true theranostic pair particularly suitable for cancer theranostics. Harnessing this potential requires development of a chelator that can rapidly form a stable complex with radioactive antimony ions at the low concentrations typical of radiopharmaceutical preparations. Stable Sb(III) complexes of hydrotris(methimazolyl)borate (TMe) are known, prompting our investigation of this chelator. Additionally, the production of radioantimony was optimized and the SPECT imaging properties of ^{117}Sb was investigated, in an attempt to move towards biomedical implementation of the theranostic isotope pair of antimony.

Results A method for rapid and effective labelling of TMe using ^{117}Sb was developed, yielding high radiochemical purities of 98.5 ± 2.7% and high radionuclidic purities exceeding 99%. Radiolabelling yielded an Sb(III) complex directly from the acidic Sb(V) solution. [^{1XX}Sb]Sb-TMe in aqueous acidic solution showed high stability in the presence of cysteine, however, the stability of the radiocomplex at increased pH was significantly decreased. The production method of ^{117}Sb was optimized, enabling a production yield of up to 19.6 MBq/μAh and the production of up to 564 MBq at end of bombardment, following irradiation of a thin ^{117}Sn-enriched solid target. Preclinical SPECT/CT scanning of a mouse phantom containing purified ^{117}Sb demonstrated excellent SPECT imaging properties of ^{117}Sb with high spatial resolution comparable to that of technetium-99m.

Conclusion We have explored the TMe chelator for complexation of radioantimony and devised a rapid chelation protocol suitable for the short half-life of ^{117}Sb ($T_{1/2}$ = 2.8 h). [^{1XX}Sb]Sb-TMe (^{1XX}Sb = ^{117}Sb, ^{118m}Sb, ^{120m}Sb and ^{122}Sb) demonstrated a high stability in presence of cysteine, although low stability was observed at pH > 4. We have achieved a production yield of ^{117}Sb high enough for clinical applications and demonstrated the excellent SPECT-imaging properties of ^{117}Sb. The results contribute valuable information for the development of suitable chelators for radioantimony and is a step further towards implementation of the antimony theranostic pair in biomedical applications.

Keywords Antimony, 119Sb, 117Sb, Scorpionate ligand, Theranostic pair, Radiolabelling, SPECT

Background

The radioisotopes of antimony (Sb), antimony-119 (^{119}Sb) and antimony-117 (^{117}Sb), have an unexploited potential as a theranostic pair for Auger electron therapy and single photon emission computed tomography (SPECT) imaging, respectively [1, 2]. As an Auger electron emitter (AEE) ^{119}Sb exhibits ideal characteristics for targeted therapy of small metastases and disseminated cancer cells. Theoretical dosimetry calculations comparing various radionuclides at a subcellular scale have identified ^{119}Sb as an isotope which should attain some of the highest calculated tumour-to-normal-tissue dose ratios, when activity is uniformly distributed in the nucleus, cytoplasm or on the cell membrane [2, 3]. It emits on average 23.7 Auger electrons (AEs) per decay [4] and has a half-life of 38.19 h, thereby offering a suitable time window for therapy. Additionally, it emits a low energy gamma ray (23.87 keV) with low intensity (16.1%), minimising the unwanted dose to healthy tissues [1]. Its sister isotope ^{117}Sb has suitable properties for SPECT imaging and can be used for diagnostics. It decays predominantly by electron capture, primarily emitting a gamma ray of 158.56 keV (86%), similar to the widely used SPECT isotope ^{123}I which emits a gamma ray of 158.97 keV (83%). Lastly, both ^{119}Sb and ^{117}Sb can be produced using a low-energy cyclotron with a solid target system. Together, they constitute a true theranostic pair possessing identical chemical properties that will result in identical kinetics, both in vitro and in vivo. Table 1 lists the physical decay characteristics of Sb radionuclides that are produced from proton bombardment of natural tin or enriched ^{117}Sn or ^{119}Sn using a low energy cyclotron.

To date, no suitable biocompatible chelating ligand system has been developed for delivering antimony. The nearly universal chelator currently implemented for metallic radionuclides, DOTA, unfortunately, does not form stable complexes with antimony [6] rendering it unsuitable for this relatively soft metal ion, the same presumably applies to the chemically related multidentate amino-carboxylato chelators based on NOTA and DPTA scaffolds. Further, we expect that the chemistry of the metalloid antimony to be intrinsically more complicated than many other metal ions used in nuclear medicine. Complexes of antimony in oxidation states + 1, +3 and + 5 have been characterised, however, it is unclear which type of compound will be sufficiently stable for medicinal use. Known complexes with antimony include the tartrate complex of Sb(III), Fig. 1(A), which is a known emetic that has previously been used to treat the tropical parasitic disease Leishmaniasis before being phased out by the pentavalent antimonial compounds sodium stibogluconate and meglumine antimoniate [7–9]. Thakur et al. have previously labelled tartrate with ^{117}Sb [10]. The low stability of this complex in vivo [11] and the lack of chemical handles for modification to enable targeting have meant that this system is unsuitable for further development as a chelator for radioantimony.

Sulfur-containing ligands are obvious choices for an exploration into the chemistry needed for application of radioantimony in nuclear medicine. Olson et al. have investigated the trithiolato ligand shown in Fig. 1(B), successfully labelling it with

Table 1 Nuclear data of selected antimony radioisotopes

Isotope	Half-life (h)	Primary decay mode (abundance)		Major γ-ray lines in keV (abundance)		Production route[a]
^{116}Sb	0.26	ε	(48%)	1293.56	(84.8%)	^{117}Sn(p,2n)^{116}Sb
		β^+	(53%)	931.81	(24.8%)	^{116}Sn(p, n)^{116}Sb
				2225.33	(14.6%)	
^{117}Sb	2.8	ε	(98.3%)	158.56	(86%)	^{117}Sn(p, n)^{117}Sb
		β^+	(1.7%)	861.35	(0.31%)	
				1004.5	(0.21%)	
^{118m}Sb	5.0	ε	(99%)	1229.68	(100%)	^{118}Sn(p, n)^{118m}Sb
		β^+	(0.2%)	253.68	(99%)	
				1050.65	(97%)	
^{119}Sb	38.2	ε	(100%)	23.87	(16.1%)	^{119}Sn(p, n)^{119}Sb
^{120m}Sb	138	ε	(100%)	1171.3	(100%)	^{120}Sn(p, n)^{120}Sb
				1023.1	(99.4%)	
				197.3	(87%)	
^{122}Sb	65.4	β^-	(97.6%)	564.12	(71%)	^{122}Sn(p, n)^{122}Sb
		ε	(2.4%)	692.79	(3.85%)	
		β^+	(0.006%)	1256.9	(0.81%)	

[a]Applicable for medical cyclotron production.

Physical decay characteristics of produced radionuclides [5] from proton bombardment of natural tin or enriched ^{117}Sn or ^{119}Sn. ε: electron capture

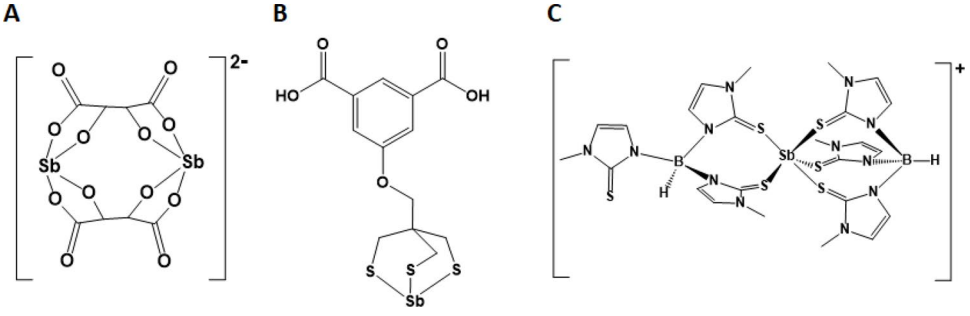

Fig. 1 Diagrams of the structures found in the single crystal X-ray structures of the antimony(III) complexes of (**A**) tartrate in Ca[Sb_2(μ-tartrato$_2$].3H_2O [14], (**B**) an isophthalic acid appended trithiolato ligand [12] and (**C**) TMe in [Sb(TMe)$_2$](TMe) [13]

^{119}Sb [12] albeit in low radiochemical yields. However, the reported dissolution and labelling methods are time consuming (>3.5 h) making it unsuitable for labelling with ^{117}Sb, due to its short 2.8 h half-life. In a new approach, we have explored the antimony chemistry and feasibility for radiolabelling of the tristhione scorpionate ligand hydrotris(methimazolyl)borate (TMe) which has been reported to form Sb(III) complexes [13], including the unsymmetrical [Sb(κ^3-TMe)(κ^2-TMe)]$^+$ cation crystallised as its TMe salt (Fig. 1(C)). Antimony chemistry is fraught by hydrolysis reactions in both the +3 and +5 state. It was therefore of some concern that [Sb(κ^3-TMe)(κ^2-TMe)]$^+$ was synthesized under non-aqueous conditions when dilute aqueous conditions at close to pH 7 will be needed for application to nuclear medicine.

In this study, we have investigated the suitability of the TMe chelator for the theranostic pair ^{119}Sb and ^{117}Sb for nuclear medicine applications. Although the use of a single multidentate chelate is typically seen as the most favourable for this application, we observe an extremely high propensity for the formation of bis homoleptic complexes and have achieved an unprecedented rapid ^{117}Sb radiolabelling.

Methods

Materials

All chemicals and solvents used were reagent grade and were used without any further purification unless otherwise stated. Chemicals used for isotope production, radiochemical separation and the radiolabeling process were all of suprapur grade or 99.99% trace metal grade, unless otherwise stated. For high performance liquid chromatography (HPLC) analysis, HPLC grade solvents were used. For Liquid chromatography-mass spectrometry (LCMS), LCMS grade solvents were used.

All water used in the radioisotope production, radiochemical separation and the radiolabelling experiments was obtained from a Milli-Q Direct-Q 3 UV system (Merck Millipore) with a resistivity of 18.2 MOhm*cm, hereafter referred to as MQ water.

Synthesis and characterisation

NaTMe

The hydrotris(3-methyl-2-thiooxoimidazolyl)borate ligand was prepared as the sodium salt (NaTMe), according to literature procedure [15].

$SbCl_2$(TMe)

NaTMe (69 mg, 0.18 mmol) was added to a MeOH (50 mL) solution of Bu_4NCl (998 mg, 3.59 mmol) which resulted in a turbid solution. This was clarified by filtration then boiled while $SbCl_3$ (42 mg, 0.18 mmol) was added slowly. An initial orange colour rapidly changed to yellow during the addition. The solution (pH = 7–8) was allowed to cool overnight resulting in the deposition of yellow crystals. These were recovered and washed with diethyl ether. Yield = 72%. $^{13}C\{^1H\}$-NMR (100 MHz, DMSO) δ (ppm) = 48.64, 13.54. ESI-MS (MeCN, pos. mode): *m/z* 239.0605 (28%, $[C_8H_{11}BN_4S_2+H]^+$ calc. 239.1420), 269.0179 (8%, $[C_4H_4ClN_2SSb]^+$ calc. 269.3600), 351.0718 (26%, $[TMe]^+$ calc. 351.2920,), 508.9352 (6.17%, $[Sb(TMe)Cl]^+$, 508.94), 825.0553 (100%, $C_{24}H_{32}B_2N_{12}S_6Sb = [Sb(TMe)_2]^+$ calc. 825.3520). ESI-MS (MeCN, neg. mode): found (calc.) m/z = 351.0678 (351.2920, 100%, $[TMe]^-$), 578.8899 (5.59%, $[Sb(TMe)Cl_3]^-$ calc. 578.88). IR (FT-ATR diamond anvil) cm^{-1} = 3050 (Csp^2-H, str, s), 1550 (C = C, str, s). Elemental analysis (%): C: 26.71; H: 3.33; N: 13.89 calc. for $C_{12}H_{16}BCl_2N_6S_3Sb$: C: 26.5; H: 2.96; N: 15.45.

[Sb(TMe)$_2$](TMe)

$K[Sb(OH)_6]$ (20 mg, 0.076 mmol) was heated in distilled water (10 mL) with stirring until dissolved. The solution was allowed to cool to approx. 50 °C before acidifying to with trifluoroacetic acid (3 drops). A solution of NaTMe (142.4 mg, 0.380 mmol) in water (3 mL) was added to the antimony solution. An orange solid precipitated during the addition and the mixture was stirred for one hour at room temperature, during which the colour of the solid changed to yellow. The yellow solid was collected by centrifugation and washed with water (3 × 8 mL), then dried under vacuum. Yield 62.2 mg, 0.53 mmol, 70.0%. ESI-MS (MeCN, pos. mode) m/z 351.06 (34%, $[C_{12}H_{16}BN_6S_3]$ + calc. 351.069), 825.05 (100%, $C_{24}H_{32}B_2N_{12}S_6Sb = [Sb(TMe)_2]^+$, calc. 825.04).

^{1}H NMR spectroscopy

Samples for were prepared in deuterated solvents and spectra were recorded on a Bruker Advance III 400 MHz spectrometer or a Jeol JNM-ECZR 500 MHz spectrometer. Data were processed with MestReNova software.

ESI Mass spectra were recorded with Electrospray ionisation (ESI) on a Bruker micrOTOF-Q II spectrometer (nanospray, capillary temperature = 180 °C, spray voltage = 3.7 kV), using acetonitrile as solvent.

UV-visible pH titration

UV-vis spectra of a solution of 0.03 mM [$Sb(TMe)_2$](TMe) in 0.1 M HCl were recorded on an Agilent 8453 spectrophotometer in 1 cm quartz cuvettes across 200–500 nm. The solution was titrated with NaOH (10 M) increasing the pH from 1.2 to 10.5 (with a MeterLab pHM240 pH meter from Radiometer Copenhagen, equipped with a Metrohm Solitrode pH-electrode).

Liquid chromatography-mass spectrometry

Liquid chromatography-mass spectrometry was performed on a Bruker Impact II UHR-TOF MS system with an Elute UHPLC system. An Intensity solo2 C18 column (100 × 2.1 mm × 2 µm) was used. A Gradient method was used (A: B, MQ water with 0.1% trifluoroacetic acid (TFA)(Sigma-Aldrich, DE): MeCN (VWR Chemicals, FR): 0–2 min: 5% B; 2–10 min: 5–95% B gradient; 10–12 min: 95% B; 12–14 min: 95−5% B gradient. Samples of NaTMe, $SbCl_2$(TMe) and [$Sb(TMe)_2$](TMe) were dissolved in MQ water with 0.1% TFA: MeCN (95:5) resulting in 0.1 mg/mL solutions.

Radioantimony production

Target preparation

^{117}Sb was produced via the ^{117}Sn(p, n)^{117}Sb nuclear reaction using highly enriched (97%) ^{117}Sn (Campro Scientific GmbH, Berlin, DE). The targets were prepared by electroplating enriched ^{117}Sn on a rhodium backing (diameter of 28 mm and thickness of 1 mm) or silver backing (diameter of 30 mm and thickness of 5 mm) as described previously [2]. Briefly, the enriched ^{117}Sn (4–6 mg) was dissolved in 30% HCl (Merck, Darmstadt, DE) containing 30% H_2O_2 (Merck, Darmstadt, DE) followed by addition of 10 M KOH (Sigma-aldrich, St. Louis, MO, USA). The solution was diluted with MQ water to 0.25 M KOH. The solution was heated and added to an electroplating cell. Electroplating was carried out with a plating current density of 7–11 mA/cm^2 for 4–5 h at a bath temperature of 70–80 °C with a platinum wire as anode.

For natural tin (^{nat}Sn) targets, 8–16 mg ^{nat}Sn (99.99% trace metals, Sigma-Aldrich, St. Louis, MO, USA) was electroplated on a rhodium backing as described above.

Target Irradiation

Electroplated tin targets were mounted in an irradiation capsule and pneumatically transferred to the cyclotron using the ARTMS QUANTM Irradiation System® ("QIS", ARTMS, Vancouver, CA) mounted on a GE PETtrace Cyclotron at the Department of Nuclear Medicine at Odense University Hospital. The GE PETtrace cyclotron was mounted with a GE aluminium energy degrader of 0.8 or 0.5 mm, reducing the proton beam energy to either ∼ 10.8 MeV or ∼ 13.1 MeV, respectively. This energy range

is within the maximum of the excitation function for the nuclear reaction ^{117}Sn(p, n)^{117}Sb [16]. ^{nat}Sn targets (12.2–18.8 mg/cm^2) were irradiated with a 10.8 MeV proton beam with beam currents of 35–40 µA for 2 h. A mixture of several long-lived radioantimony isotopes primarily comprising ^{118m}Sb, ^{120m}Sb and ^{122}Sb as well as ^{117}Sb (combined denoted ^{1XX}Sb in the following) were produced by proton bombardment of ^{nat}Sn and used for subsequent radiolabelling experiments. Enriched ^{117}Sn targets (3.73–8.03 mg/cm^2) were irradiated with either 10.8 or 13.1 MeV proton beams with a beam current of 40 µA for 45–60 min.

Beam current ramping

A beam current ramping experiment with 13.1 MeV protons was performed to investigate the cooling properties of a 20.3 mg/cm^2 ^{nat}Sn target. Proton beam currents of up to 55 µA were tested. Visual inspection of the target was performed between each beam current increment, to determine whether melting of the target was occurring.

Radiochemical separation

Dissolution of irradiated tin targets and radiochemical separation of ^{117}Sb or ^{1XX}Sb from the target material was performed as described previously [17]. Briefly, tin targets were dissolved in 700 µL warm (~ 40°C) 30% HCl containing 50–100 µL 30% H_2O_2. After 10 min, 50 µL 30% H_2O_2 was added to ensure complete oxidation followed by an increase in temperature to ~ 60°C (in the solution) to ensure decomposition of the remaining H_2O_2. When bubbles stopped forming, the solution was transferred to a column (1.0 × 15 cm) packed with AG 4-X4 anion exchange resin (100–200 mesh, free base form, BIO-RAD, USA) preconditioned with 0.8 M HCl. Radioantimony was eluted with 0.8 M HCl (flowrate of 0.8 mL/min) and collected in plastic vials. The radiochemical separation was monitored using a shielded NaI detector to measure the count rate in the eluate in the exit tube as a function of eluant volume. To evaluate the separation yield and radionuclidic purity (RNP) of the radioantimony fraction, collected samples were measured using a calibrated broad-energy Ge detector (BEGE2020-7600SL; Canberra) with detector software Genie 2000 (version 3.2.1; Canberra). Radioantimony isotopes were identified and quantified according to the γ-lines listed in Table S1.

Radiolabelling and quality control

A sample of the purified radioantimony fraction was mixed with 2.8 mM NaTMe (dissolved in MQ water) in a 1:5 ratio (V/V), the solution was left for 45–60 min at room temperature. The radiochemical purity (RCP) of the radioantimony labelled TMe complex ([^{117}Sb]Sb-TMe and [^{1XX}Sb]Sb-TMe), was determined by analytical reverse-phase (RP) HPLC on a Hitachi LaChrom Elite system with diode array detection in series with radio-detection and a Phenomenex Gemini C18 column (150 × 4.6 mm, 5 µm, 0.7 mL/min). The same gradient program used for LCMS was used with MQ water with 0.1% TFA (Sigma-Aldrich, FR) and acetonitrile (VWR Chemicals, FR) as eluent. Non-radioactive $SbCl_2$(TMe) dissolved in MQ water (0.9 mM) was added to all samples containing radiolabelled complex (1:1 V/V) before they were run on HPLC, to limit adsorption of the radiocomplex on the HPLC column. Nevertheless, small but detectable amounts of radioantimony remained on the HPLC column after elution and the resulting RCP values are thereby guiding and not quantitative.

Stability experiments

Cysteine challenge

[^{1XX}Sb]Sb-TMe was prepared as described above. 100 µL of the radiolabelling solution (0.22±0.01 MBq, 4.0 MBq/µmol, n=3) was diluted in 500 µL of 25 mM cysteine (pH 5, Sigma-Aldrich, St. Louis, MO, USA) dissolved in MQ water. The pH was 0–1 after mixing with cysteine. The solutions were incubated at 37 °C for up to 48 h. Samples were drawn after 0, 24 and 48 h. The samples were analysed by RP-HPLC, as previously described, to determine the RCP. The RCP was also determined prior to mixing with cysteine, 45–60 min after the addition of TMe.

pH-dependent stability

[^{1XX}Sb]Sb-TMe was prepared as previously described. The RCP was assessed 45–60 min after the addition of TMe to radioantimony, by performing RP-HPLC analysis as previously described. Subsequently, the pH of the radiolabelling solution was increased with NaOH (Sigma-Aldrich, UK) until reaching pH 6–7. RP-HPLC analysis was then immediately performed to assess the RCP. It should be noted that HPLC-analysis was performed under acidic conditions, hence the pH of the sample was likely reduced when the sample was analysed.

SPECT/CT imaging with ^{117}Sb

The NEMA NU 4-2008 Phantom (NU4IQ) comprising one main phantom body with two cold inserts and 5 fillable rods with inner diameters of 1, 2, 3, 4 and 5 mm [18], was used to investigate the suitability of ^{117}Sb as a SPECT isotope in a preclinical setting. Purified ^{117}Sb was thoroughly mixed with MQ water and was added to the phantom. SPECT/CT scanning of the phantom was performed on a Siemens INVEON multimodality pre-clinical scanner (Siemens pre-clinical solutions, Knoxville, TN, USA). The phantom contained 74.4 MBq ^{117}Sb at the beginning of the SPECT/CT scan.

The SPECT/CT protocol included first a 2-bed CT scan obtained for attenuation correction and structural orientation. The CT was obtained with the following settings: half rotation, 180 projections, 4 × 4 bin, and low magnification covering the entire phantom. The exposure settings were 80 kV and 500 µA at 250ms. The CT scan was reconstructed using the Feldkamp algorithm, with a Sheep-Logan filter, slight noise reduction, and Hounsfield calibration.

The SPECT scan was performed using two synchronized detectors with general-purpose mouse collimators (MGP-1.0). The acquisition parameters included a 35 mm radius of rotation, 60 projections/revolution, 1.0 revolution, 6° angle, and 300 s/step resulting in a total scan time of 5 h 48 min. The energy window was 143–175 kV with a photopeak at 159 kV. CT and SPECT images were co-registered using a transformation matrix, and the SPECT data was reconstructed using an MAP3D algorithm (matrix 128 × 128, 8 iterations, and 6 subsets) with a requested resolution of 1.4 mm. Attenuations correction and scatter correction was applied and the SPECT/CT data were analyzed using the dedicated imaging analysis software Inveon Research Workplace (Siemens Medical Solutions Malvern, PA, USA).

For comparison, SPECT/CT scans of the known SPECT isotope, technetium-99m (^{99m}Tc) were also performed under the same conditions, with few alterations. For acquisition 228 s/projection was applied to comply with the longer half-life of ^{99m}Tc ($T_{1/2}$ =

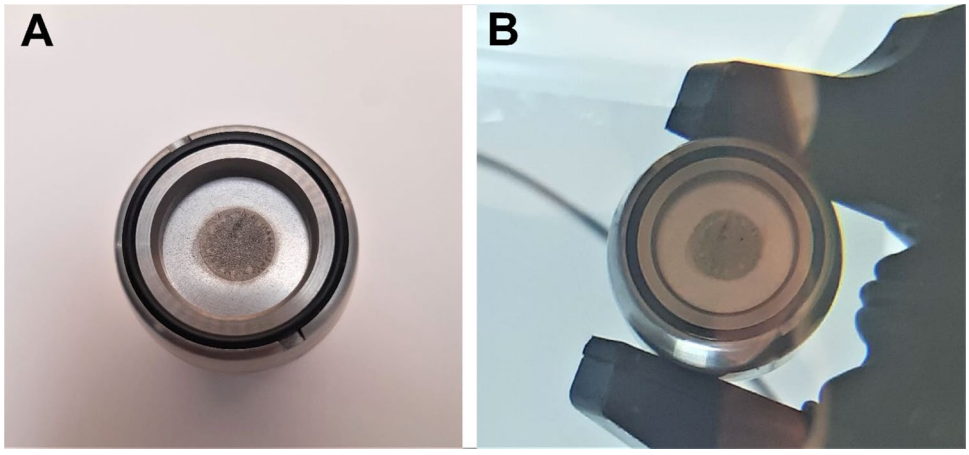

Fig. 2 Natural tin target before (**A**) and after (**B**) irradiation with 13.1 MeV protons and a beam current of 45 µA

Table 2 Irradiation of ^{nat}Sn targets

Beam current (µA)	Total charge (µAh)	Target thickness (mg / cm^2)	Measured production yield (MBq/µAh)	Calculated production yield for 97% enriched ^{117}Sn target (MBq/µAh)
40	79.6	17.9	4.7	59.3
40	79.6	12.2	2.3	29.6
35	69.1	18.8	3.4	42.7

Production details including beam current, total charge, target thicknesses of natural tin targets, ^{117}Sb production yields at end of bombardment after irradiation with a 10.8 MeV proton beam and production yields calculated for a corresponding target with 97% tin-117 enrichment

6.01 h), resulting in a total scan time of 3 h and 48 min. The phantom contained 72.3 MBq ^{99m}Tc at the beginning of the SPECT/CT scan.

Statistics

Results are presented as mean ± standard deviation (SD) when $n \geq 3$.

Results

Radioantimony production

Beam current ramping

The beam current ramping experiment showed that the electroplated ^{nat}Sn target (20.3 mg/cm^2) could withstand beam currents of up to at least 45 µA of 13.1 MeV protons with no sign of visual damage (Fig. 2) of the tin layer. At 55 µA protons, however, some melting of the tin was observed. Hence, the target could withstand an average power density of more than 0.75 kW/cm^2.

^{1XX}Sb production

Following the beam ramping experiment, ^{nat}Sn targets (12.2–18.8 mg/cm^2) were irradiated for 2 hours with a 10.8 MeV proton beam and a beam current of 40 µA. The longer irradiation time of 2 hours was tested to see if the targets could withstand it. Production yields of ^{117}Sb at end of bombardment of ^{nat}Sn targets are listed in Table 2 (with produced activities listed in Table S2). ^{nat}Sn targets withstood irradiations of up to 2 hours without showing any sign of melting and resulted in ^{117}Sb production yields of up to 4.7

MBq/μAh. This would correspond to a production yield of up to 59.3 MBq/μAh if an enriched (97%) ^{117}Sn target of the same thickness had been irradiated.

^{117}Sb production

Irradiation of enriched ^{117}Sn targets with beam currents of 10.8 (n=3) and 13.1 MeV (n=1) resulted in production yields of 12.4–19.6 and 14.3 MBq/μAh, respectively. All productions of ^{117}Sb at both 10.8 MeV and 13.1 MeV resulted in similar radionuclidic purities of 92.4–94.8%. The remaining 7.6-5.2% corresponded to the short-lived antimony-116 (^{116}Sb, $T_{1/2}$ = 15.8 min). The biggest ^{117}Sb production resulted in 564 MBq of ^{117}Sb with a radionuclidic purity of 94.8% at end of bombardment. The separation was performed in 120 min (including 45 min of cooling time to allow decay of ^{116}Sb) and resulted in the collection of 205 MBq ^{117}Sb. At end of separation (EOS), no radionuclidic impurities were detected (RNP=100%), for any ^{117}Sb production. An overview of the ^{117}Sb production details is shown in Table 3. The table includes production yields calculated from cross sections found in literature [16, 19–21] for the listed target thicknesses and the beam energy used. It is evident from Table 3 that the measured production yield constitute 56–67% of the theoretical production yield.

Based on experimental and theoretical cross sections published in literature [16, 19–21] (extracted from graphical plots), a thick target yield for the ^{117}Sn(p, n)^{117}Sb nuclear reaction in the 15→8 MeV range was calculated to be 1.48 GBq/μAh. In practice, this would correspond to 0.83–0.99 GBq/μAh for the production conditions used above, as indicated by the difference between the measured and theoretical production yields presented in Table 3.

Synthesis and characterisation of cold Sb complexes of TMe

The methods section contains the preparations and spectroscopic data for the isolated non-radioactive solid state Sb compounds $SbCl_2$(TMe) and [Sb(TMe)$_2$](TMe). ESI MS (Fig. S1) and LCMS data (Fig. S2 and S3) suggest that, in solution, the predominant antimony species present is [Sb(TMe)$_2$]$^+$ regardless of whether $SbCl_2$(TMe) or [Sb(TMe)$_2$](TMe) was dissolved. The crystal structure of [Sb(TMe)$_2$](TMe) has been reported previously [13] (CCDC 274857). Further studies of the solid state and rich solution chemistry of these and related Sb(III) complexes with TMe will be reported in due course.

TMe radiolabelling and quality control

TMe was successfully radiolabelled with radioactive antimony. RP-HPLC analysis of [^{1XX}Sb]Sb-TMe, after 60 min of incubation at room temperature, showed one clear peak

Table 3 Irradiation of enriched ^{117}Sn targets

Beam energy (MeV)	Beam current (μA)	Total charge (μAh)	Target thickness (mg / cm^2)	Measured production yield (MBq/μAh)	Theoretical production yield (MBq/μAh)
10.8	30	22.2	5.0	12.4	22.1
10.8	30	22.1	8.0	19.6	32.9
10.8	40	29.7	5.4	12.5	22.1
13.1	40	39.6	3.7	14.3	21.2

Production details including beam energy, beam current, total charge, target thickness, production yield of ^{117}Sb and theoretical production yields based on experimental cross sections found in literature [16, 19–21] following irradiation of enriched ^{117}Sn targets with a proton beam of 10.8 or 13.1 MeV

in the radio chromatogram with a retention time of 10.9 min (Fig. S4.A). The corresponding peak also dominates the UV chromatogram at 10.9 min (Fig. S4.B), which has the same elution time as the peak observed when performing RP-HPLC analysis of non-radioactive $SbCl_2$(TMe) (Fig. S5). The absence of non-chelated ^{1XX}Sb, which elutes after 2.75 min (Fig. S6), suggested complete radiolabelling of TMe. Radiolabelling of TMe with ^{1XX}Sb yielded a RCP of 99.5 ± 1.0% (n = 4) following incubation for 1 h at room temperature. Radiolabelling of TMe with ^{117}Sb resulted in the formation of [^{117}Sb]Sb-TMe with a high RCP of 98.5 ± 2.7% (8.8–33.0 MBq/µmol, n = 3), 45 min after the addition of radioantimony (Fig. 3).

Stability experiments

The stability of the [^{1XX}Sb]Sb-TMe complex was examined in presence of cysteine for 48 h at pH 1. The stability was assessed by determining the RCP by RP-HPLC analysis, which was measured to be >99% throughout 48 h (Fig. 4.A). No degradation of the complex or dissociation of radioantimony was observed by HPLC. The stability of the ^{1XX}Sb-radiolabelled complex was investigated at a higher pH by increasing the pH of the radiolabelling solution to 6-7 and then performing radio HPLC-analysis (Fig. 4.B). A decrease of >95% of the RCP was observed after increasing the pH of the radiolabelling solution.

Ultraviolet-visible light pH titration of [Sb(TMe)$_2$](TMe)

The stability of the non-radioactive [Sb(TMe)$_2$](TMe) complex in an aqueous solution was investigated by ultraviolet-visible light (UV-vis) pH titration. Solutions of [Sb(TMe)$_2$](TMe) were yellow below approximately pH 3 indicating coordination by thione sulfur atoms and that the complex cation was intact. This is supported by LCMS showing the dominant 823 m/z ion for [Sb(TMe)$_2$]$^+$ (Fig. S2). Titration of a solution of [Sb(TMe)$_2$](TMe) at pH 1 with NaOH (Fig. 5) revealed that bleaching was complete at

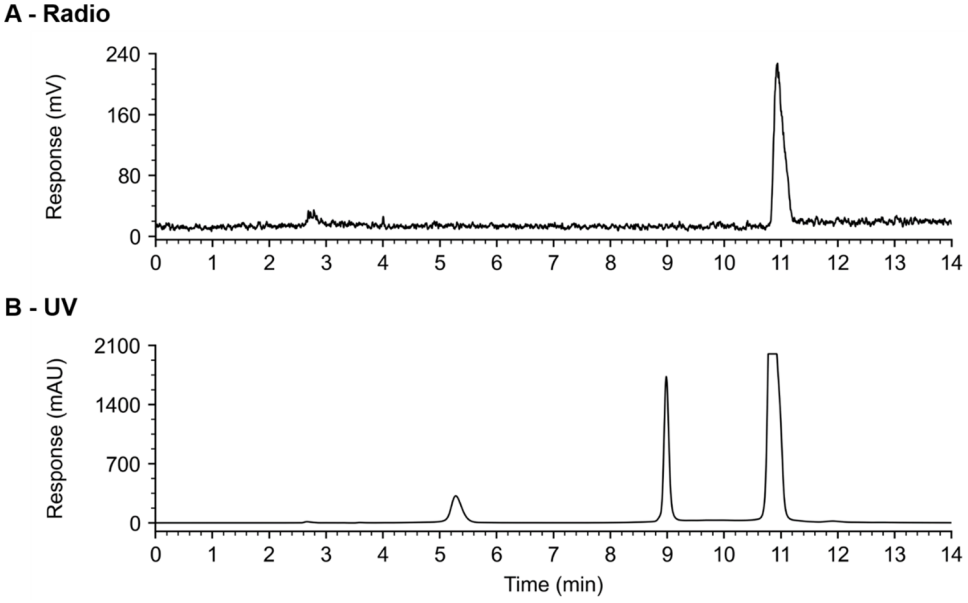

Fig. 3 (**A**) radio chromatogram and (**B**) UV chromatogram obtained from analytical RP-HPLC of a sample of [^{117}Sb]Sb-TMe (13.3 MBq/µmol) mixed (1:1 V/V) with 0.9 mM non-radioactive Sb(TMe)Cl_2 dissolved in MQ water

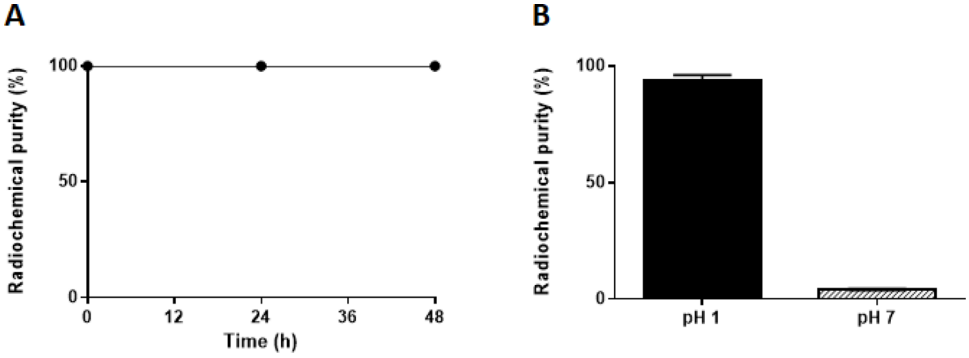

Fig. 4 (**A**): Stability of the [^{1XX}Sb]Sb-TMe complex in 21 mM cysteine for up to 48 h ($n = 3$). pH after mixing was 0–1. Radiochemical purity was determined by radio HPLC analysis. (**B**): Radiochemical purity of TMe labelled with ^{1XX}Sb at pH 1 (black) and immediately after increasing the pH of the radiolabelling solution to 6-7 (grey stripes), ($n = 3$). All samples were mixed (1:1 V/V) with 0.9 mM non-radioactive $SbCl_2$(TMe) dissolved in MQ water (pH 5) prior to RP-HPLC analysis. Data is presented as mean ± SD

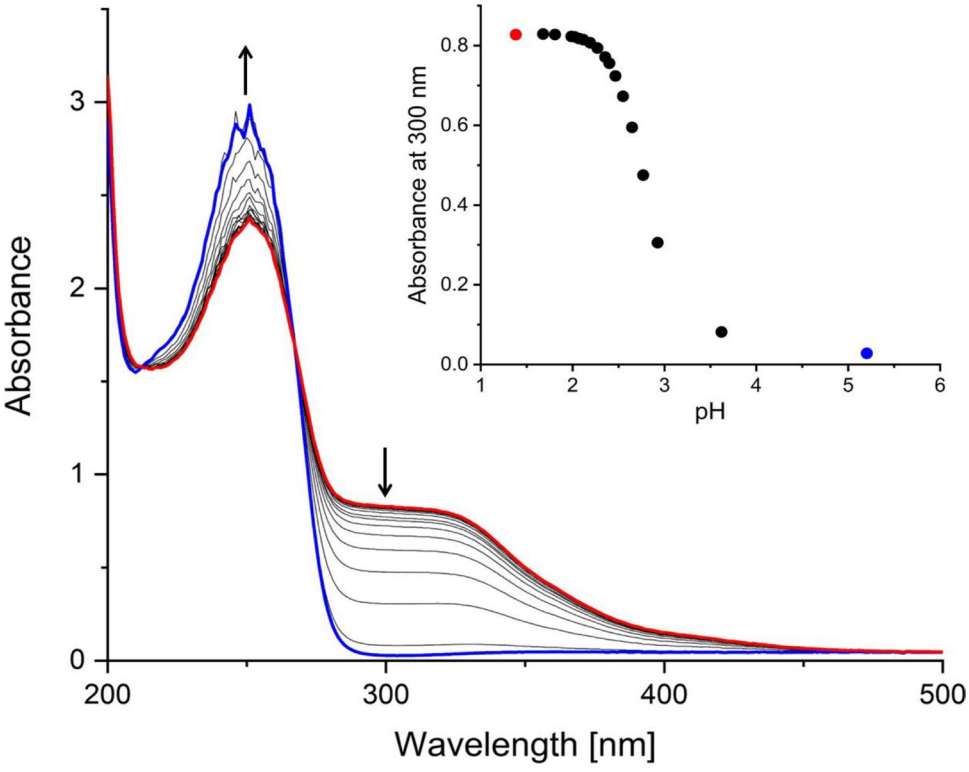

Fig. 5 UV-VIS spectrum of a solution of [Sb(TMe)(TMe)](TMe) (0.03 mM) dissolved in 0.1 M HCl and titrated with NaOH. Insert: decrease in the intensity of the shoulder at 300 nm with increasing pH

pH 4 (Fig. 5). The final UV-vis spectrum is identical to that of an aqueous solution of the free ligand, showing absorption maxima at 250 nm and no absorption above 300 nm.

SPECT/CT imaging

In order to verify the suitability of ^{117}Sb as a SPECT isotope, its imaging abilities were assessed by performing a SPECT/CT scan of the NU4IQ phantom containing purified ^{117}Sb using a preclinical SPECT/CT scanner. Scans and depictions of the phantom are shown in Fig. 6. All rods could be located on the scans (Fig. 6.A.1 and D), but the

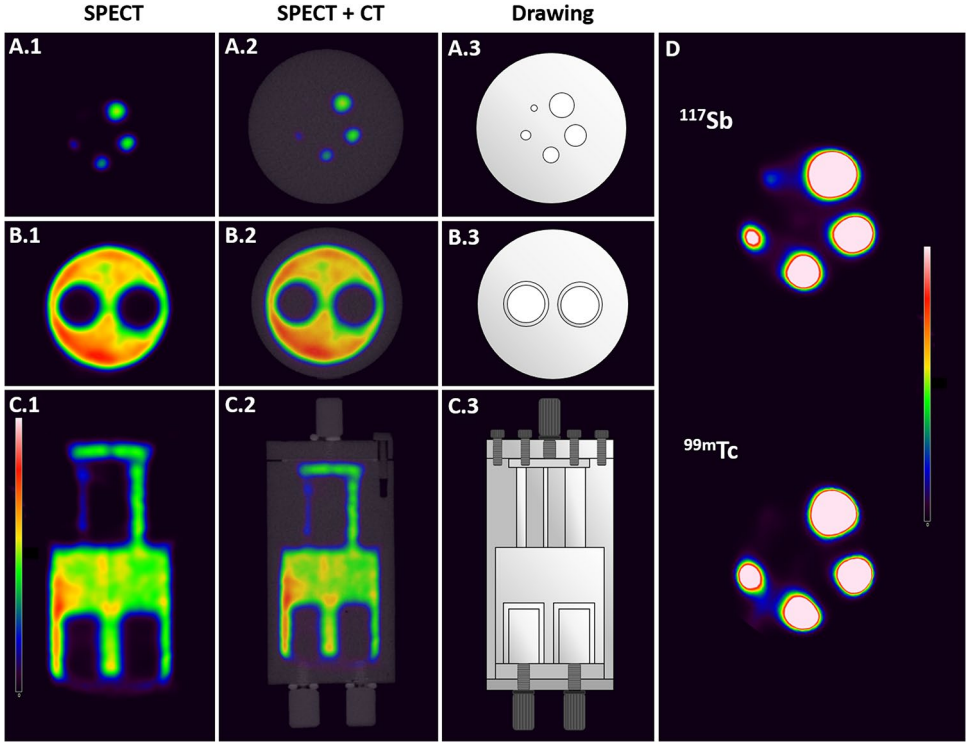

Fig. 6 (1) SPECT and (2) SPECT/CT of the NU4IQ Phantom containing ^{117}Sb. (3) drawings of the NU4IQ Phantom. (**A**): axial slice of the five radioactive rods of 1, 2, 3, 4 and 5 mm in diameter. (**B**): axial slice of the two chambers containing water (8 mm). (**C**): coronal slice. (**D**): SPECT images of the five rods (axial) with a higher intensity scale for the scan performed with ^{117}Sb and a scan performed with ^{99m}Tc for comparison, at the same intensity scale

smallest rod (1 mm) was only just discernible. The two non-radioactive inserts were visible as well (Fig. 6.B).

SPECT/CT scans of the NU4IQ Phantom with the clinically used ^{99m}Tc was performed, as depicted in Fig. 6.D, using the same intensity scale as for the ^{117}Sb SPECT image for comparison. All rods were distinguishable, similarly to the ^{117}Sb SPECT-scan, however, the smallest rod was less discernible than for ^{117}Sb.

Discussion

The potentially highly potent Auger electron emitter ^{119}Sb and the SPECT-isotope ^{117}Sb form an isotope pair particularly suitable for cancer theranostics. The great potential of this true theranostic pair and the lack of suitable chelators for antimony highlights a need for chelators that form stable complexes with antimony using a simple and rapid labelling method, compatible with the short half-life of ^{117}Sb. In this study, we introduce TMe as a potential chelator for complexing ^{119}Sb and ^{117}Sb.

Radioantimony production

High beam current irradiation of electroplated tin metal is challenged by the low melting point of tin (232 °C). To our knowledge, we successfully conducted the highest beam current irradiations of tin metal on a commercially available, fully automated solid target system, without melting of the target material. This optimization of the radioantimony production method enabled the achievement of a production yield of up to 19.6 MBq/μAh using a biomedical cyclotron. Following irradiation of a thin solid target (3.7 mg/

cm^2) for 1 h with a 13.1 MeV proton beam at a beam current of 40 µA, 564 MBq of ^{117}Sb was produced at end of bombardment (EOB). Using a target thickness of 20 mg/cm^2 as performed in the beam current ramping experiment and extending the irradiation time to 2 hours, would lead to the production of approx. 6 GBq of ^{117}Sb at EOB. Taking into account the radiochemical yield of the Sn/Sb separation, almost 3.5 GBq would be available for labelling at EOS. Should an appropriate chelator with fast complexation kinetics < 1 h, be used, then the resulting activity levels should be adequate for several clinical examinations. Even higher activities (> 50 GBq) can be obtained by increasing the target thickness. The activity yield was calculated from published cross sections, while considering the 33–47% lower practical yield observed in this work. After radiochemical separation, radiolabelling, and quality control, the amount of ^{117}Sb produced would be enough activity for tens of patients at several hospitals, if a dose of 200 MBq per patients was estimated, which is more than adequate for clinical applications. It should be noted that, although the thin targets used in this work could withstand a beam current of up to 45 µA, a thicker target might not be able to withstand such a high beam current due to the low thermal conductivity of tin and thus, poorer cooling. This limitation could potentially be avoided by using an inclined target/beam geometry with a larger surface area irradiated and lower physical thickness of the tin layer, thereby ensuring an effective cooling of the target. It has previously been reported that the use of an inclined beam enabled irradiation of a 10 mg/cm^2 ^{nat}Sn target with a 150 µA proton beam current for up to 76 min [22]. The described production and separation method underlines the feasibility of readily producing ^{117}Sb via solid target irradiation with biomedical cyclotrons found in hospitals, resulting in activity yields of ^{117}Sb adequate for clinical applications.

SPECT/CT imaging with ^{117}Sb

Establishing the suitability of ^{117}Sb as a SPECT isotope is essential if it is to be used with ^{119}Sb as a true theranostic pair. Using a theranostic pair consisting of the same element offers advantages in terms of displaying identical pharmacokinetics, biodistribution and the same affinity towards a given molecular target. Changing the radioisotope-chelator complex, as for theranostic pairs from different elements, has been reported to change the pharmacokinetics of the radiopharmaceuticals, limiting their use as a theranostic pair [23–25]. Although theranostic pairs of different elements are used in the clinic, e.g. gallium-68 and lutetium-177 used for patient selection and treatment, respectively, for patients with metastatic castration-resistant prostate cancer [26], using a theranostic pair of the same element is far more advantageous as it enhances the imaging and therapy compatibility. The purified ^{117}Sb was used for SPECT/CT scans of a NU4IQ phantom, to determine its suitability as a SPECT isotope. The images shown in Fig. 6 are, to our knowledge, the first reported SPECT/CT images with ^{117}Sb performed on a preclinical scanner. The SPECT/CT scan of the phantom demonstrated excellent spatial resolution, all radioactive rods could be identified, and the visibility of the non-radioactive inserts was retained. The spatial resolution of the ^{117}Sb images was slightly better than the images obtained with the clinically used ^{99m}Tc, as the lowest diameter rod (1 mm) was barely distinguishable when a higher intensity scale was applied for the ^{99m}Tc SPECT scan, demonstrating the great SPECT-imaging properties of ^{117}Sb. The remarkable SPECT imaging properties of ^{117}Sb combined with the simple and highly

implementable production method that enables the isolation of several GBq's of purified ^{117}Sb, locally at the hospital, underline its potential as a future clinical SPECT isotope.

TMe radiolabelling

HPLC-analysis of [^{117}Sb]Sb-TMe combined with the LCMS studies of aqueous solutions of Sb-TMe complexes, suggests that TMe was successfully radiolabelled with ^{117}Sb forming the bis-complex [[^{117}Sb]Sb(TMe)$_2$]$^+$ observed in aqueous solution. TMe was readily labelled through simple mixing under acidic conditions at room temperature and yielded high RCPs of 98.5 ± 2.7% within 45 min post ^{117}Sb addition. The radioantimony is reduced from its +5 to +3 oxidation state during the reaction. The most likely reducing agent in this reaction is the ligand itself, known to readily undergo oxidative degradation, forming several decomposition products [27, 28]. Although resulting in oxidative degradation of some of the excess TMe present, this did not affect the RCP, as evidenced by the absence of other radio-signals in the HPLC radio chromatograms and the achievement of a high RCP. This stresses the remarkable properties of TMe as a chelator for radioantimony.

Cysteine challenge and stability tests

The successful radiolabelling of TMe prompted an investigation of the stability of [^{1XX}Sb]Sb-TMe. [^{1XX}Sb]Sb-TMe showed high stability in cysteine for 48 h, with no observable decrease in the RCP, suggesting no release of radioantimony from TMe was occurring under acidic conditions. However, raising the pH of the radiolabelling solution led to substantial instability instantaneously, with a pronounced release of radioantimony exceeding 95%, despite the sample being analysed by HPLC under acidic conditions, as the eluent used has a pH of about 1. Nevertheless, the instability was reversible, as lowering the pH to 1 resulted in an increase in RCP if left for a few hours. Reported thermodynamic equilibrium predictions of antimony in water matrices showed reversible hydrolysis of Sb(III) occurring at pH 1 (~ 20%), forming Sb(OH)$_3$ and reaching almost 100% above pH 4 [29]. This suggests that the instability of [^{1XX}Sb]Sb-TMe at a higher pH originated from hydrolysis of radioantimony upon increasing the pH. This is consistent with the instability observed when performing UV-vis pH titration of a solution of non-radioactive [Sb(TMe)$_2$](TMe) at pH 1 with NaOH. The UV-spectra revealed decoordination of antimony from the TMe ligands due to hydrolysis and formation of colourless Sb(OH)$_3$ was complete at pH 4. Given the current absence of suitable chelators for radioantimony, these findings provide crucial insights into the host design for radioantimony advancing efforts to establish the antimony theranostic pair for medical applications.

Conclusions

Through optimization of the production method for ^{117}Sb, we successfully attained a high production yield, facilitating the generation of a sufficient quantity of ^{117}Sb for clinical applications. Notably, we report the first SPECT/CT scanning of a mouse phantom containing purified ^{117}Sb performed by a preclinical scanner. This demonstrates the excellent SPECT imaging properties of ^{117}Sb with high spatial resolution comparable to that of ^{99m}Tc. The soft anionic scorpionate ligand hydrotris(3-methyl-2-thiooxoimidazolyl)borate, TMe, is able to complex ^{117}Sb(V) rapidly in acidic solution to yield a radiolabelled Sb(III) complex in one synthetic step. The radiocomplex, proposed to be [^{117}Sb]

$Sb(TMe)_2]^+$, showed high stability in the presence of high concentrations of cysteine for 48 h. The stability of the radiocomplex at physiological pH was low, presumably due to extensive hydrolysis of the complexed radioantimony. Despite stability challenges of the radiocomplex at neutral pH, this work contributes to advancing the establishment of the antimony theranostic pair for biomedical applications.

Abbreviations

AE	Auger electron
AEE	Auger electron emitter
EOB	End of bombardment
EOS	End of separation
ESI	Electrospray ionisation
HPLC	High performance liquid chromatography
LCMS	Liquid chromatography-mass spectrometry
MeCN	Acetonitrile
MS	Mass spectrometry
NU4IQ	NEMA NU 4-2008 Phantom
RCP	Radiochemical purity
RNP	Radionuclidic purity
RP	Reverse-phase
SD	Standard deviation
SPECT	Single-photon emission computed tomography
TFA	Trifluoroacetic acid
TMe	hydrotris(methimazolyl)borate

Supplementary Information

The online version contains supplementary material available at https://doi.org/10.1186/s41181-024-00297-5.

Supplementary Material 1

Acknowledgements
Not applicable.

Authors contributions
Conceptualization methodology and project administration was performed by LG, HT, CJM, VM and JD. Hands-on work was performed by LG, MM, VM, CC and VC. Data analysis was performed by LG, HT, CJM, VM, MM, NL and JD. Manuscript editing was performed by LG, HT, CJM, VM, NL and MM. First draft writing was performed by LG. All authors read and approved the final manuscript.

Funding
The work presented in this paper was supported by the NovoNordisk Foundation Interdisciplinary Synergy Programme 2022 (NNF22OC0077099).

Data availability
The datasets used and/or analyzed during the current study are available from the corresponding author on reasonable request.

Declarations

Ethics approval and consent to participate
Not applicable.

Consent for publication
Not applicable.

Competing interests
The authors declare that they have no competing interests.

Received: 12 June 2024 / Accepted: 10 September 2024
Published online: 05 November 2024

References

1. Filosofov D, Kurakina E, Radchenko V. Potent candidates for targeted Auger Therapy: production and radiochemical considerations. Nucl Med Biol. 2021;94–95:1–19.
2. Thisgaard H, Jensen M. 119Sb–a potent Auger emitter for targeted radionuclide therapy. Med Phys. 2008;35(9):3839–46.

3. Uusijärvi H, Bernhardt P, Ericsson T, Forssell-Aronsson E. Dosimetric characterization of radionuclides for systemic tumor therapy: influence of particle range, photon emission, and subcellular distribution. Med Phys. 2006;33(9):3260–9.
4. Ku A, Facca VJ, Cai Z, Reilly RM. Auger electrons for cancer therapy – a review. EJNMMI Radiopharmacy Chem. 2019;4(1):27.
5. Chu SYF, Ekström LP, Firestone RB. The Lund/LBNL Nuclear Data Search, Version 2.0 1999 http://nucleardata.nuclear.lu.se/toi/index.asp. Accessed 20 Feb. 2024.
6. Chen C, Sommer C, Thisgaard H, McKee V, McKenzie CJ. Facile transmetallation of [SbIII(DOTA)] – renders it unsuitable for medical applications. RSC Adv. 2022;12(10):5772–81.
7. Brahmachari UN. Chemotherapy of antimonial compounds in kala-azar infection. Part IV. Further observations on the therapeutic values of urea stibamine. By U.N., Brahmachari. 1922. Indian J Med Res. 1989;89:393–404.
8. Haldar AK, Sen P, Roy S. Use of Antimony in the treatment of Leishmaniasis: current status and future directions. Mol Biology Int. 2011;2011:571242.
9. Aronson N, Herwaldt BL, Libman M, Pearson R, Lopez-Velez R, Weina P, et al. Diagnosis and treatment of Leishmaniasis: clinical practice guidelines by the Infectious Diseases Society of America (IDSA) and the American Society of Tropical Medicine and Hygiene (ASTMH). Am J Trop Med Hyg. 2017;96(1):24–45.
10. Thakur ML, Clark JC, Silvester DJ. The production of 117Sb-labelled potassium antimonyl tartrate for medical use. Int J Appl Radiat Isot. 1970;21(1):33–6.
11. Sun H, Yan SC, Cheng WS. Interaction of antimony tartrate with the tripeptide glutathione. Eur J Biochem. 2000;267(17):5450–7.
12. Olson AP, Ma L, Feng Y, Najafi Khosroshahi F, Kelley SP, Aluicio-Sarduy E, et al. A third generation potentially bifunctional trithiol chelate, its nat,1XXSb(III) complex, and selective chelation of radioantimony (119Sb) from its Sn Target. Inorg Chem. 2021;60(20):15223–32.
13. Dodds CA, Reglinski J, Spicer MD. Lower main-group element complexes with a soft scorpionate ligand: the structural influence of stereochemically active Lone pairs. Chem – Eur J. 2006;12(3):931–9.
14. Gress ME, Jacobson RA. X-ray and white radiation neutron diffraction studies of optically active potassium antimony tartrate, K2Sb2(d-C4H2O6)2·3H2O (tarter emetic). Inorg Chim Acta. 1974;8:209–17.
15. Reglinski J, Garner M, Cassidy I D, Slavin A, Spicer PD, Armstrong MR. D. Sodium hydrotris(methimazolyl)borate, a novel soft, tridentate ligand: preparation, structure and comparisons with sodium hydrotris(pyrazolyl)borate. J Chem Soc Dalton Trans. 1999(13):2119–26.
16. Zherebchevsky VI, Alekseev IE, Lazareva TV, Maltsev NA, Nauruzbayev DK, Nesterov DG, et al. New Radionuclides for Personalized Medicine. Bull Russian Acad Sciences: Phys. 2021;85(10):1128–35.
17. Thisgaard H, Jensen M. Production of the Auger emitter 119Sb for targeted radionuclide therapy using a small PET-cyclotron. Appl Radiat Isot. 2009;67(1):34–8.
18. NEMA standards publication NU. 4-2008: performance measurements of small animal positron emission tomographs. Rosslyn, VA: National Electrical Manufacturers Association; 2008.
19. Batij VG, Skakun EA. Cross sections of the (p,n) reactions on the 117,118,122,124Sn. Nuclear spectroscopy an nuclear structure. Summaries of reports of the 41. International conference; 1991; USSR.
20. Klyucharev AP, Skakun EA, Rakivnenko YN, Romanii IA. Excitation functions of (p,n) reactions on some Sn isotopes and the Isomeric Cross Section Ratios. Soviet J Nuclear Phys. 1970;11:530.
21. Lovchikova GN, Sal'nikov OA, Simakov SP, Trufanov AM, Kotel'nikova GV, Pilz V et al. Study of the mechanism of the reactions 94Zr(p,n) 94Nb, 119Sn(p,n)119Sb, and 122Sn(p,n) 122Sb in the proton energy range 6–9 MeV. Sov J Nucl Phys (Engl Transl); (United States). 1980;31:1:1–5.
22. Thisgaard H, Jensen M, Elema DR. Medium to large scale radioisotope production for targeted radiotherapy using a small PET cyclotron. Appl Radiat Isot. 2011;69(1):1–7.
23. Miller C, Rousseau J, Ramogida CF, Celler A, Rahmim A, Uribe CF. Implications of physics, chemistry and biology for dosimetry calculations using theranostic pairs. Theranostics. 2022;12(1):232–59.
24. Mitran B, Thisgaard H, Rinne S, Dam J, Azami F, Tolmachev V, et al. Selection of an optimal macrocyclic chelator improves the imaging of prostate cancer using cobalt-labeled GRPR antagonist RM26. Sci Rep. 2019;9:17086.
25. Deshmukh MV, Voll G, Kühlewein A, Mäcke H, Schmitt J, Kessler H, et al. NMR studies reveal structural differences between the Gallium and Yttrium complexes of DOTA-d-Phe-Tyr3-octreotide. J Med Chem. 2005;48(5):1506–14.
26. Fallah J, Agrawal S, Gittleman H, Fiero MH, Subramaniam S, John C et al. FDA approval summary: Lutetium Lu 177 Vipivotide Tetraxetan for patients with metastatic castration-resistant prostate cancer. Clin Cancer Res. 2023;29(9):1651–7.
27. Spicer MD, Reglinski J. Soft Scorpionate ligands based on Imidazole-2-thione donors. Eur J Inorg Chem. 2009;2009(12):1553–74.
28. Rajasekharan-Nair R, Marckwordt A, Lutta ST, Schwalbe M, Biernat A, Armstrong DR, et al. Soft Scorpionate anions as platforms for Novel Heterocycles. Chem – Eur J. 2013;19(40):13561–8.
29. Mitrakas M, Mantha Z, Tzollas N, Stylianou S, Katsoyiannis I, Zouboulis A. Removal of Antimony species, Sb(III)/Sb(V), from Water by using Iron coagulants. Water. 2018;10(10):1328.

Publisher's note